

Distributed Optimal Frequency Control Considering a Nonlinear Network-Preserving Model

Zhaojian Wang, Feng Liu, John Z. F. Pang, Steven Low, *Fellow, IEEE* and Shengwei Mei, *Fellow, IEEE*

Abstract—This paper addresses the distributed optimal frequency control of power systems considering a network-preserving model with nonlinear power flows and excitation voltage dynamics. Salient features of the proposed distributed control strategy are fourfold: i) nonlinearity is considered to cope with large disturbances; ii) only a part of generators are controllable; iii) no load measurement is required; iv) communication connectivity is required only for the controllable generators. To this end, benefiting from the concept of “virtual load demand”, we first design the distributed controller for the controllable generators by leveraging the primal-dual decomposition technique. We then propose a method to estimate the virtual load demand of each controllable generator based on local frequencies. We derive incremental passivity conditions for the uncontrollable generators. Finally, we prove that the closed-loop system is asymptotically stable and its equilibrium attains the optimal solution to the associated economic dispatch problem. Simulations, including small and large-disturbance scenarios, are carried on the New England system, demonstrating the effectiveness of our design.

Index Terms—Frequency control, network-preserving model, distributed control, incremental output passivity

I. INTRODUCTION

Frequency restoration and economic dispatch (ED) are two important problems in power system operation. Conventionally, they are implemented hierarchically in a centralized fashion, where the former is addressed in a fast time scale while the latter in a slow time scale [1], [2]. While this centralized hierarchy works well for the traditional power system, it may not be able to keep pace with the fast development of our power system due to: 1) slow response, 2) insufficient flexibility, 3) low privacy, 4) intense communication, and 5) single point of failure issue. In this regard, the idea of breaking such a hierarchy is proposed in [3], [4].

In [5], an intrinsic connection between the asymptotic stability of the dynamical frequency control system with the ED problem is proposed. It leads to a so-called inverse-engineering methodology for designing optimal frequency controllers, where the (partial) primal-dual gradient algorithm

plays an essential role [1], [6]. When designing optimal frequency controllers, in choice of power flow models, including the linear model (usually associated with DC power flow, e.g. [5], [7]–[15]) and the nonlinear model (usually associated with AC power flow, e.g. [16]–[21]), is crucial. While the closed-loop system can be interpreted in a linear model as carrying out a primal-dual algorithm for solving ED, this interpretation of frequency control may not hold in a nonlinear model. In addition to nonlinear power flow, excitation voltage dynamics are considered in [16]–[18], making the model more realistic.

The aforementioned idea is further developed to enable the design of distributed optimal frequency controllers. Roughly speaking, the works of distributed optimal frequency control can be divided into two categories in terms of different power system models: network-reduced models e.g. [5], [12]–[16], [18] and network-preserving models e.g. [7]–[11], [17]. In network-reduced models, generators and/or loads are aggregated and treated as one bus or control area, which are connected to each other through tie lines. In [5], [13], aggregated generators in each area are driven by automatic generation control (AGC) to restore system frequency. [12], [14]–[16], [18] further consider both the aggregated generators and load demands in frequency control. In network-preserving models, generator and load buses are separately handled with different dynamic models and coupled by power flows, rendering a set of differential algebraic equations (DAEs). In [7], an optimal load control (OLC) problem is formulated and a primary load-side control is derived as a partial primal-dual gradient algorithm for solving the OLC problem. The design approach is extended to secondary frequency control (SFC) that restores nominal frequency in [8]. It is generalized in [9], where passivity condition guaranteeing stability is proposed for each local bus. Then, a unified framework combining load and generator control is advocated in [10]. A similar model is also utilized in [11], where only limited control coverage is needed. Similar to [18], the Hamiltonian method is used to analyze the network-preserving model in [17]. Compared with the network-reduced model, the network-preserving model describes power systems more precisely and appear more suitable for analyzing interactions between different control areas. Therefore, we specifically consider the network-preserving model in this work.

Almost all of aforementioned works assume that all buses are controllable and load demands at all buses are accurately measurable, especially for those proposing secondary frequency control. Moreover, it is usually assumed that the communication network has the same topology of the power grid. These assumptions are strong and arguably unrealistic

This work was supported by the National Natural Science Foundation of China (No. 51677100, U1766206, No. 51621065), the US National Science Foundation through awards EPCN 1619352, CCF 1637598, CNS 1545096, ARPA-E award de-ar0000699, and Skoltech through Collaboration Agreement 1075-MRA. (Corresponding author: Shengwei Mei)

Z. Wang, F. Liu and S. Mei are with the State Key Laboratory of Power System and Department of Electrical Engineering, Tsinghua University, Beijing, China, 100084. e-mail: (meishengwei@mail.tsinghua.edu.cn).

S. H. Low and J. Pang are with the Department of Electrical Engineering, California Institute of Technology, Pasadena, CA, USA, 91105. e-mail: (slow@caltech.edu).

for practice. First, only a part of generators and controllable load buses can participate in frequency control in practice. Second, the communication network may not be identical to the topology of the power grid. Third, it is difficult to accurately measure the load injection on every bus. In extreme cases, even the number of load buses is unknown in practice. These problems highlight some reasons why theoretical work in this area is hardly applied in practical systems.

In this context, a novel distributed frequency recovery controller is proposed that only needs to be implemented on controllable generator buses. To this end, a network-preserving power system model is adopted. This work is an extension of our former work [11]. However, in this paper, we design a totally different controller considering a third-order nonlinear generator model with excitation voltage dynamics and nonlinear power flow. It is also motivated partly by [17], which adopts a similar model, although our results are significantly different from those in [17]. Differing from [11], the controller avoids load measurement, which greatly facilitates implementation. By using LaSalle's invariance principle, it is proved that the closed-loop system converges to an equilibrium point that solves the economic dispatch problem. The salient features of the proposed distributed optimal frequency controller are:

- 1) *Model*: The network-preserving model of power system is used, including excitation voltage dynamics and nonlinear power flow. This, unlike work on the linear model, returns a valid controller even under large disturbances.
- 2) *Controllability*: We allow an arbitrary subset of generator buses to be controllable.
- 3) *Controller*: The distributed controller achieves the optimal solution to economic dispatch while restoring the nominal frequency, provided that certain sufficient conditions on active power dynamics of uncontrollable generators and excitation voltage dynamics of all generators are satisfied.
- 4) *Communication*: Communication is required between neighboring controllable generators only, and the communication network can be arbitrary as long as it remains connected.
- 5) *Measurement*: No load measurement is needed, and the controller is adaptive to unknown load changes.

The rest of this paper is organized as follows. In Section II, we introduce the power system model. Section III formulates the optimal economic dispatch problem. The distributed controller is proposed in Section IV, and we further prove the optimality and stability of the corresponding equilibrium point in Section V. The load estimation method is proposed in Section VI. We confirm the performance of controllers via simulations on a detailed power system in Section VII. Section VIII concludes the paper.

II. POWER SYSTEM MODELS

A. Power Network

Power systems are composed of many generators and loads, which are integrated in different buses and connected by power lines, forming a power network. Buses are divided into three types, controllable generator buses, uncontrollable generator

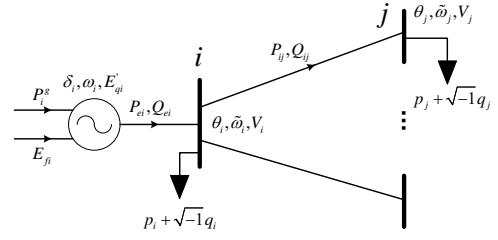


Fig. 1. Summary of notations

buses and pure load buses. Denote controllable generator buses as $\mathcal{N}_{CG} = \{1, 2, \dots, n_{CG}\}$, uncontrollable generator buses as $\mathcal{N}_{UG} = \{n_{CG} + 1, n_{CG} + 2, \dots, n_{CG} + n_{UG}\}$, and pure load buses as $\mathcal{N}_L = \{n_{CG} + n_{UG} + 1, \dots, n_{CG} + n_{UG} + n_L\}$. Then the set of generator buses is $\mathcal{N}_G = \mathcal{N}_{CG} \cup \mathcal{N}_{UG}$ and set of all the buses is $\mathcal{N} = \mathcal{N}_G \cup \mathcal{N}_L$. It should be noted that load can be connected to any bus besides pure load buses.

Let $\mathcal{E} \subseteq \mathcal{N} \times \mathcal{N}$ be the set of lines, where $(i, j) \in \mathcal{E}$ if buses i and j are connected directly. Then the whole system is modeled as a connected graph $\mathcal{G} = (\mathcal{N}, \mathcal{E})$. The admittance of each line is $Y_{ij} := G_{ij} + \sqrt{-1}B_{ij}$ with $G_{ij} = 0$ for every line. Denote the bus voltage by $V_i \angle \theta_i$, where V_i is the amplitude and θ_i is the voltage phase angle. The active and reactive power P_{ij}, Q_{ij} from bus i to bus j is

$$P_{ij} = V_i V_j B_{ij} \sin(\theta_i - \theta_j) \quad (1a)$$

$$Q_{ij} = B_{ij} V_i^2 - V_i V_j B_{ij} \cos(\theta_i - \theta_j) \quad (1b)$$

For convenience, most notations are summarized in Fig.1.

B. Synchronous Generators

For $i \in \mathcal{N}_G$, we use the standard third-order generator model (e.g. [18], [22], [23]) (2a)-(2c). Here (2d) is the simplified governor-turbine model, and (2e) is the excitation voltage control model:

$$\dot{\delta}_i = \omega_i \quad (2a)$$

$$\dot{\omega}_i = (P_i^g - D_i \omega_i - P_{ei}) / M_i \quad (2b)$$

$$\dot{E}'_{qi} = -E_{qi} / T'_{d0i} + E_{fi} / T'_{d0i} \quad (2c)$$

$$\dot{P}_i^g = -P_i^g / T_i + u_i^g \quad (2d)$$

$$\dot{E}_{fi} = h(E_{fi}, E_{qi}) \quad (2e)$$

In this model, M_i is the moment of inertia; D_i the damping constant; T'_{d0i} the d -axis transient time constant; T_i the time constant of turbine; δ_i the power angle of generator i ; ω_i the generator frequency deviation compared to a steady state value; P_i^g the mechanical power input; p_j the active load demand; P_{ei} the active power injected to network; E'_{qi} the q -axis transient internal voltage; E_{qi} the q -axis internal voltage; E_{fi} the excitation voltage. E_{qi} is given by

$$E_{qi} = \frac{x_{di}}{x'_{di}} E'_{qi} - \frac{x_{di} - x'_{di}}{x'_{di}} V_i \cos(\delta_i - \theta_i) \quad (3)$$

where x_{di} is the d -axis synchronous reactance, and x'_{di} is the d -axis transient reactance.

The active and reactive power (denoted by Q_{ei}) injection to the network are

$$P_{ei} = \frac{E'_{qi} V_i}{x'_{di}} \sin(\delta_i - \theta_i) \quad (4a)$$

$$Q_{ei} = \frac{V_i^2}{x'_{di}} - \frac{E'_{qi} V_i}{x'_{di}} \cos(\delta_i - \theta_i) \quad (4b)$$

For controllable generators $i \in \mathcal{N}_{CG}$, the capacity limits are

$$\underline{P}_i^g \leq P_i^g \leq \bar{P}_i^g \quad (5)$$

where $\underline{P}_i^g, \bar{P}_i^g$ are lower and upper limits of P_i^g .

C. Dynamics of Voltage Phase Angles

To build a network-preserving power system model, relation between generators and power network should be explicitly established. In this paper, loads for bus $i \in \mathcal{N}$ are simply modeled as constant active and reactive power injections. Then the following equations are used to dictate the power balance and voltage phase-angle dynamics at each bus:

$$\dot{\theta}_i = \tilde{\omega}_i, \quad i \in \mathcal{N} \quad (6a)$$

$$0 = P_{ei} - \tilde{D}_i \tilde{\omega}_i - p_i - \sum_{j \in N_i} P_{ij}, \quad i \in \mathcal{N}_G \quad (6b)$$

$$0 = -\tilde{D}_i \tilde{\omega}_i - p_i - \sum_{j \in N_i} P_{ij}, \quad i \in \mathcal{N}_L \quad (6c)$$

$$0 = Q_{ei} - q_i - \sum_{j \in N_i} Q_{ij}, \quad i \in \mathcal{N}_G \quad (6d)$$

$$0 = -q_i - \sum_{j \in N_i} Q_{ij}, \quad i \in \mathcal{N}_L \quad (6e)$$

where, p_i, q_i are active and reactive load demands, respectively; $\tilde{\omega}_i$ the frequency deviation at bus i ; N_i the set of buses connected directly to bus i ; \tilde{D}_i the damping constant at bus i ; $\tilde{D}_i \tilde{\omega}_i$ the change of frequency-sensitive load [7].

In power system, line power flows are mainly related to power angle difference between two buses rather than the power angles independently. Then, we define new variables to denote angle differences as $\eta_{ii} := \delta_i - \theta_i, i \in \mathcal{N}_G$ and $\eta_{ij} := \theta_i - \theta_j, i, j \in \mathcal{N}$. The time derivative of η_{ii} and η_{ij} are

$$\dot{\eta}_{ii} = \omega_i - \tilde{\omega}_i, \quad i \in \mathcal{N}_G \quad (7a)$$

$$\dot{\eta}_{ij} = \tilde{\omega}_i - \tilde{\omega}_j, \quad i, j \in \mathcal{N}, i \neq j \quad (7b)$$

respectively. In the following analysis, we use η_{ii} and η_{ij} as new state variables instead of δ_i and θ_i .

To summarize, (1)–(4), (6b)–(6e), (7a), (7b) constitute the nonlinear network preserving model of power systems, which is in a form of differential-algebraic equations (DAE).

D. Communication Network

In this paper, we consider a communication graph among the buses of controllable generators only. Denote $E \subseteq \mathcal{N}_{CG} \times \mathcal{N}_{CG}$ as the set of communication links. If generator i and j can communicate directly to each other, we denote $(i, j) \in E$. Obviously, edges in the communication graph E can be different from lines in the power network \mathcal{E} . For the communication network, we make the following assumption:

A1: The communication graph E is undirected and connected.

III. FORMULATION OF OPTIMAL FREQUENCY CONTROL

A. Optimal Power-Sharing Problem in Frequency Control

The purpose of optimal frequency control is to let all the controllable generators share power mismatch economically when restoring frequency. Then we have the following optimization formulation, denoted by SFC.

$$\text{SFC: } \min_{P_i^g, i \in \mathcal{N}_{CG}} \sum_{i \in \mathcal{N}_{CG}} f_i(P_i^g) \quad (8a)$$

$$\text{s.t. } \sum_{i \in \mathcal{N}_{CG}} P_i^g = \sum_{i \in \mathcal{N}} p_i - \sum_{i \in \mathcal{N}_{UG}} P_i^{g*} \quad (8b)$$

$$\underline{P}_i^g \leq P_i^g \leq \bar{P}_i^g, \quad i \in \mathcal{N}_{CG} \quad (8c)$$

where P_i^{g*} is the mechanical power of uncontrollable generator in the steady state. In (8a), $f_i(P_i^g)$ concerns the controllable generation P_i^g , satisfying the following assumption:

A2: The objective $f_i(P_i^g)$ is second-order continuously differentiable, strongly convex and $f'_i(P_i^g)$ is Lipschitz continuous with Lipschitz constant $l_i > 0$. i.e. $\exists \alpha_i > 0, \alpha_i \leq f''_i(P_i^g) \leq l_i$.

To ensure the feasibility of the optimization problem, we make an additional assumption.

A3: The system satisfies

$$\sum_{i \in \mathcal{N}_{CG}} \underline{P}_i^g \leq \sum_{i \in \mathcal{N}} p_i - \sum_{i \in \mathcal{N}_{UG}} P_i^{g*} \leq \sum_{i \in \mathcal{N}_{CG}} \bar{P}_i^g \quad (9)$$

Specifically, we say A3 is *strictly satisfied* if all the inequalities in (9) *strictly* hold.

B. Equivalent Optimization Model with Virtual Load Demands

In (8b), load demands are injected to every bus, which sometimes cannot be measured accurately if at all. As a consequence, the values of p_i may be unknown to both the controllable generators $i, i \in \mathcal{N}_{CG}$ and the uncontrollable generators $i, i \in \mathcal{N}_{UG}$. To circumvent such an obstacle in design, we introduce a set of new variables, \hat{p}_i , to re-formulate SFC as the following equivalent problem:

$$\text{ESFC: } \min_{P_i^g, i \in \mathcal{N}_{CG}} \sum_{i \in \mathcal{N}_{CG}} f_i(P_i^g) \quad (10a)$$

$$\text{s.t. } \sum_{i \in \mathcal{N}_{CG}} P_i^g = \sum_{i \in \mathcal{N}_{CG}} \hat{p}_i \quad (10b)$$

$$\underline{P}_i^g \leq P_i^g \leq \bar{P}_i^g, \quad i \in \mathcal{N}_{CG} \quad (10c)$$

where \hat{p}_i is the *virtual load demand* supplied by generator i in the steady state, which is a constant, satisfying $\sum_{i \in \mathcal{N}_{CG}} \hat{p}_i = \sum_{i \in \mathcal{N}} p_i - \sum_{i \in \mathcal{N}_{UG}} P_i^{g*}$. Obviously, the number of virtual loads should be equal to that of the controllable generators.

Note that the power balance constraint (8b) only requires that all the generators supply all the loads while it is not necessary to figure out which loads are supplied exactly by which generators. Hence we treat virtual load demands \hat{p}_i as the effective demands supplied by generator i for dealing with the issue that only a part of generators are controllable.

Simply letting $\sum_{i \in \mathcal{N}_{CG}} \hat{p}_i = \sum_{i \in \mathcal{N}} p_i - \sum_{i \in \mathcal{N}_{UG}} P_i^{g*}$, we immediately have the following Lemma:

Lemma 1. The problems SFC (8) and ESFC (10) have the same optimal solutions.

IV. CONTROLLER DESIGN

A. Distributed Frequency Control of Controllable Generators

1) *Controller design based on primal-dual gradient algorithm*: Invoking the primal-dual gradient algorithm, the Lagrangian of the ESFC (10) is given by

$$L = \sum_{i \in \mathcal{N}_{CG}} f_i(P_i^g) + \mu \left(\sum_{i \in \mathcal{N}_{CG}} P_i^g - \sum_{i \in \mathcal{N}_{CG}} \hat{p}_i \right) + \gamma_i^- (P_i^g - \underline{P}_i^g) + \gamma_i^+ (P_i^g - \overline{P}_i^g), \quad i \in \mathcal{N}_{CG} \quad (11)$$

where $\mu, \gamma_i^-, \gamma_i^+$ are Lagrangian multipliers. Based on primal-dual update, the controller for $i \in \mathcal{N}_{CG}$ is designed as

$$u_i^g = P_i^g/T_i - k_{P_i^g} \left(\omega_i + (f'_i(P_i^g) + \mu - \gamma_i^- + \gamma_i^+) \right) \quad (12a)$$

$$\dot{\mu} = k_\mu \left(\sum_{i \in \mathcal{N}_{CG}} P_i^g - \sum_{i \in \mathcal{N}_{CG}} \hat{p}_i \right) \quad (12b)$$

$$\dot{\gamma}_i^- = k_{\gamma_i} [P_i^g - \underline{P}_i^g]_{\gamma_i^-}^+ \quad (12c)$$

$$\dot{\gamma}_i^+ = k_{\gamma_i} [P_i^g - \overline{P}_i^g]_{\gamma_i^+}^- \quad (12d)$$

where $k_{P_i^g}, k_\mu, k_{\gamma_i}$ are positive constants; u_i^g the control input; $f'_i(P_i^g)$ the marginal cost at P_i^g . For any $x_i, a_i \in \mathbb{R}$, the operator is defined as: $[x_i]_{a_i}^+ = x_i$ if $a_i > 0$ or $x_i > 0$; and $[x_i]_{a_i}^+ = 0$ otherwise.

2) *Estimating μ by second-order consensus*: In (12b), μ is a global variable, which is a function of mechanical powers and loads of the entire system. To circumvent the obstacle in implementation, a second-order consensus based method is utilized to estimate μ locally by using neighboring information only. Specifically, for $i \in \mathcal{N}_{CG}$, the controller is revised to:

$$u_i^g = P_i^g/T_i - k_{P_i^g} \left(\omega_i + f'_i(P_i^g) + \mu_i - \gamma_i^- + \gamma_i^+ \right) \quad (13a)$$

$$\dot{\mu}_i = k_{\mu_i} \left(P_i^g - \hat{p}_i - \sum_{j \in \mathcal{N}_{ci}} (\mu_i - \mu_j) - \sum_{j \in \mathcal{N}_{ci}} z_{ij} \right) \quad (13b)$$

$$\dot{z}_{ij} = k_{z_{ij}} (\mu_i - \mu_j) \quad (13c)$$

$$\dot{\gamma}_i^- = k_{\gamma_i} [P_i^g - \underline{P}_i^g]_{\gamma_i^-}^+ \quad (13d)$$

$$\dot{\gamma}_i^+ = k_{\gamma_i} [P_i^g - \overline{P}_i^g]_{\gamma_i^+}^- \quad (13e)$$

where, $k_{\mu_i}, k_{z_{ij}}$ are positive constants; \mathcal{N}_{ci} the set of neighbors of bus i in the communication graph; μ_i the local estimation of μ . Here, (13b) and (13c) are used to estimate μ locally, where only neighboring information is needed. z_{ij} is an auxiliary variable to guarantee the consistency of all μ_i .

For the Lagrangian multiplier μ , $-\mu$ is often regarded as the marginal cost of generation. Theoretically, $-\mu_i$ should reach consensus for all the generators in the steady state. Since $\dot{\mu}_i = 0$ holds in the steady state, we have $P_i^g - \hat{p}_i - \sum_{j \in \mathcal{N}_{ci}} z_{ij} = 0$. Hence, z_{ij} can be regarded as the virtual line power flow of edge (i, j) in the communication graph.

B. Active Power Dynamics of Uncontrollable Generators

To guarantee system stability, a sufficient condition is given for the active power dynamics of uncontrollable generators.

C1: The active power dynamics of uncontrollable generators are strictly incrementally output passive in terms of the

input $-\omega_i$ and output P_i^g , i.e., there exists a continuously differentiable, positive semidefinite function S_{ω_i} such that

$$\dot{S}_{\omega_i} \leq (-\omega_i - (-\omega_i^*)) (P_i^g - P_i^{g*}) - \phi_{\omega_i} (P_i^g - P_i^{g*})$$

where ϕ_{ω_i} is a positive definite function, and $\phi_{\omega_i} = 0$ holds only when $P_i^g = P_i^{g*}$.

The condition C1 on the active power dynamics of uncontrollable generators is easy to verify. As an example, the commonly-used primary frequency controller

$$u_i^g = -\omega_i + \omega_i^* - k_{\omega_i} (P_i^g - P_i^{g*}) + P_i^g/T_i \quad (14)$$

satisfies C1 whenever $k_{\omega_i} > 0$. In this case, we have $S_{\omega_i} = \frac{k_1}{2} (P_i^g - P_i^{g*})^2$ with $k_1 > 0$ and $\phi = k_2 (P_i^g - P_i^{g*})^2$ with $0 < k_2 \leq k_{\omega_i} \cdot k_1$.

C. Excitation Voltage Dynamics of All Generators

Similar to the uncontrollable generators, the following sufficient condition on excitation voltage dynamics of all generators is needed to guarantee system stability, since we do not design specific excitation voltage controllers here.

C2: The excitation voltage dynamics are strictly incrementally output passive in terms of the input $-E_{qi}$ and output E_{fi} , i.e., there exists continuously differentiable, positive semidefinite function S_{E_i} such that

$$\dot{S}_{E_i} \leq (-E_{qi} - (-E_{qi}^*)) (E_{fi} - E_{fi}^*) - \phi_{E_i} (E_{fi} - E_{fi}^*)$$

where ϕ_{E_i} is a positive definite function, and $\phi_{E_i} = 0$ holds only when $E_{fi} = E_{fi}^*$.

C2 is also easy to satisfy. As an example, it can be verified that the controller given in [23]

$$h(E_{fi}, E_{qi}) = -E_{fi} + E_{fi}^* - k_{E_i} (E_{qi} - E_{qi}^*) \quad (15)$$

with $k_{E_i} > 0$ satisfies C2. In this case, $S_{E_i} = \frac{k_3}{2} (E_{fi} - E_{fi}^*)^2$ with $k_3 > 0$ and $\phi = k_4 (E_{fi} - E_{fi}^*)^2$ with $0 < k_4 \leq k_{E_i} \cdot k_3$.

V. OPTIMALITY AND STABILITY

After implementing the controller on the physical power system, the closed-loop system reads

$$\begin{cases} (1) - (4), (6b) - (6e), (7a), (7b) \\ (13a) - (13e) \end{cases} \quad (16)$$

In this section, we prove the optimality and stability of the closed-loop system (16).

A. Optimality

Denote the trajectory of closed-loop system as $v(t) = (\eta(t), \omega(t), \tilde{\omega}(t), P^g(t), \mu(t), z(t), \gamma^-(t), \gamma^+(t), E_q'(t), V(t))$. Define the equilibrium set of (16) as

$$\mathcal{V} := \{v^* | v^* \text{ is an equilibrium of (16)}\} \quad (17)$$

We first present the following Theorem.

Theorem 2. Suppose assumptions A1, A2 and A3 hold. In equilibrium of (16), following assertions are true.

- 1) The mechanical powers P_i^g satisfy $\underline{P}_i^g \leq P_i^g \leq \overline{P}_i^g$, $\forall i \in \mathcal{N}_{CG}$.

- 2) System frequency recovers to the nominal value, i.e. $\omega_i^* = 0, \forall i \in \mathcal{N}_{CG} \cup \mathcal{N}_{UG}$, and $\tilde{\omega}_i^* = 0, \forall i \in \mathcal{N}$.
- 3) The marginal generation costs satisfy $f'_i(P_i^{g*}) - \gamma_i^{-*} + \gamma_i^{+*} = f'_j(P_j^{g*}) - \gamma_j^{-*} + \gamma_j^{+*}, i, j \in \mathcal{N}_{CG}$.
- 4) P_i^{g*} is the unique optimal solution of SFC problem (8).
- 5) μ_i^* is unique if A3 is strictly satisfied.

The detailed proof of Theorem 2 is given in Appendix.A of this paper. It shows that the nominal frequency is recovered at equilibrium, and marginal generation costs are identical for all controllable generators, implying the optimality of any equilibrium.

B. Stability

In this section, the stability of the closed-loop system (16) is proved. First we define a function as

$$\begin{aligned} \hat{L} := & \sum_{i \in \mathcal{N}_{CG}} f_i(P_i^{g*}) + \sum_{i \in \mathcal{N}_{CG}} \mu_i(P_i^g - \hat{p}_i) \\ & - \sum_{i \in \mathcal{N}_{CG}} \mu_i z_{ij} - \frac{1}{2} \sum_{i \in \mathcal{N}_{CG}} \left(\mu_i \sum_{j \in \mathcal{N}_i} (\mu_i - \mu_j) \right) \\ & + \sum_{i \in \mathcal{N}_{CG}} \gamma_i^- (P_i^g - \bar{P}_i^g) + \sum_{i \in \mathcal{N}_{CG}} \gamma_i^+ (P_i^g - \bar{P}_i^g) \end{aligned} \quad (18)$$

Denote $x_1 := (P^g)$, $x_2 := (\mu, z, \gamma_i^-, \gamma_i^+)$, $x := (x_1, x_2)$. Then $\hat{L}(x_1, x_2)$ is convex in x_1 and concave in x_2 .

Before giving the main result, we construct a Lyapunov candidate function composed of four parts: the quadratic part, the potential energy part, conditions C1 and C2 related parts, as we now explain.

For $i \in \mathcal{N}_G$, the quadratic part is given by

$$W_k(\omega, x) = \sum_{i \in \mathcal{N}_G} \frac{1}{2} M_i (\omega_i - \omega_i^*)^2 + \frac{1}{2} (x - x^*)^T K^{-1} (x - x^*) \quad (19)$$

where $K = \text{diag}(k_{P_i^g}, k_{\mu_i}, k_{z_i}, k_{\gamma_i})$ is a diagonal positive definite matrix.

Denoting $x_p = (E'_{qi}, V_i, \delta_i, \theta_i)$, the potential energy part is

$$W_p(x_p) = \tilde{W}_p(x_p) - (x_p - x_p^*)^T \nabla_{x_p} \tilde{W}_p(x_p^*) - \tilde{W}_p(x_p^*) \quad (20)$$

where,

$$\begin{aligned} \tilde{W}_p(E'_{qi}, V_i, \delta_i, \theta_i) = & \sum_{i \in \mathcal{N}} \frac{1}{2} B_{ii} V_i^2 + \sum_{i \in \mathcal{N}} p_i \theta_i \\ & - \sum_{i \in \mathcal{N}} q_i \ln V_i - \frac{1}{2} \sum_{i \in \mathcal{N}} \sum_{j \in \mathcal{N}_i} V_i V_j B_{ij} \cos(\theta_i - \theta_j) \\ & - \sum_{i \in \mathcal{N}_G} \frac{E'_{qi} V_i}{x'_{di}} \cos(\delta_i - \theta_i) + \sum_{i \in \mathcal{N}_G} \frac{x_{di}}{2x'_{di}(x_{di} - x'_{di})} \left(E'_{qi} \right)^2 \end{aligned} \quad (21)$$

Conditions C1 and C2 related parts are $\sum_{i \in \mathcal{N}_{UG}} S_{\omega_i}$ and $\sum_{i \in \mathcal{N}_G} \frac{1}{T'_{d0i}(x_{di} - x'_{di})} S_{E_i}$ respectively.

The Lyapunov function is defined as

$$W = W_k + W_p + \sum_{i \in \mathcal{N}_{UG}} S_{\omega_i} + \sum_{i \in \mathcal{N}_G} \frac{S_{E_i}}{T'_{d0i}(x_{di} - x'_{di})} \quad (22)$$

Then, we give the following assumption.

A4: The Hessian of W_p satisfies $\nabla_v^2 W_p(v) > 0$ at desired equilibrium.

Since the voltage phase deviation between two neighboring buses is not large in practice, A4 is usually satisfied. Detailed explanations can be found in Appendix.B of this paper.

The following stability result can be obtained.

Theorem 3. Suppose A1–A4 and C1, C2 hold. For every v^* , there exists a neighborhood \mathcal{S} around v^* where all trajectories $v(t)$ satisfying (16) starting in \mathcal{S} converge to the set \mathcal{V} . In addition, each trajectory converges to an equilibrium point.

We can further prove that $\nabla^2 W > 0$ and $\dot{W} \leq 0$. Moreover, $\dot{W} = 0$ holds only at equilibrium point. Then the theorem can be proved using the LaSalle's invariance principle [24, Theorem 4.4]. Details of the proof are given in Appendix.B.

VI. IMPLEMENTATION BASED ON FREQUENCY MEASUREMENT

A. Estimation and Optimality

Note that virtual load demands \hat{p}_i used in the controller (13) are difficult to directly measure or estimate in practice. Lemma 1 implies that any \hat{p}_i are valid as long as $\sum_{i \in \mathcal{N}_{CG}} \hat{p}_i = \sum_{i \in \mathcal{N}} P_i - \sum_{i \in \mathcal{N}_{UG}} P_i^{g*}$. Noticing that the power imbalance is very small in normal operation, we have $\sum_{i \in \mathcal{N}_{CG}} P_{ei} \approx \sum_{i \in \mathcal{N}} \hat{p}_i$. In fact, they are identical in steady state. Hence, we specify $\hat{p}_i = P_{ei}$, which implies $P_i^g - \hat{p}_i = P_i^g - P_{ei} = M_i \dot{\omega}_i + D_i \omega_i$. That leads to an estimation algorithm of μ_i

$$\begin{aligned} \dot{\mu}_i = & k_{\mu_i} \left(- \sum_{j \in \mathcal{N}_i} (\mu_i - \mu_j) - \sum_{j \in \mathcal{N}_i} z_{ij} + M_i \dot{\omega}_i + D_i \omega_i \right. \\ & \left. + \tau_i (-\mu_i - f'_i(P_i^g) + \gamma_i^- - \gamma_i^+) \right) \end{aligned} \quad (23)$$

where $0 < \tau_i < 4/l_i$. This way, we only need to measure frequencies ω_i at each bus locally, other than the global load demands. Since the controller only needs μ_i of neighboring buses in the communication graph, it is easy to implement.

Now, we reconstruct the closed-loop system by replacing (13b) with (23) in (16), which is

$$\begin{cases} (1) - (4), (6b) - (6e), (7a), (7b) \\ (13a), (13c) - (13e), (23) \end{cases} \quad (24)$$

We have the following lemma.

Lemma 4. Assertions 1)-5) in Theorem 2 still hold for the equilibrium of (24).

The proof of Lemma 4 is given in Appendix.C.

B. Discussion on Stability

Recall (2b), then (23) is derived to

$$\begin{aligned} \dot{\mu}_i = & k_{\mu_i} \left(P_i^g - \hat{p}_i + \hat{p}_i - P_{ei} - \sum_{j \in \mathcal{N}_i} (\mu_i - \mu_j) - \sum_{j \in \mathcal{N}_i} z_{ij} \right. \\ & \left. + \tau_i (-\mu_i - f'_i(P_i^g) + \gamma_i^- - \gamma_i^+) \right) \end{aligned} \quad (25)$$

Denote $\rho_i = \hat{p}_i - P_{ei} = P_{ei}^* - P_{ei}$, which is the difference of electric power and its value in the steady state. We have the following assumption

A5: The disturbance can be written as $\rho_i = \beta_i(t) \omega_i$, where $|\beta_i(t)| \leq \beta_i$ and β_i is a positive constant. In addition, the set $\{ t < \infty \mid \omega_i(t) = \omega_i^* \}$ has a measure zero.

Whenever $\omega_i \neq \omega_i^*$, there always exists such $\beta_i(t)$. A5 argues that $\omega_i(t) = \omega_i^*$ only happens at isolated points except equilibrium. Generally, this is reasonable in power system.

Denote the state variables of (24) and its equilibrium set are \tilde{v} and \tilde{V} respectively. We have following stability result

Theorem 5. Suppose A1–A5, C1, C2 hold and (9) is not binding. For every \tilde{v}^* , there exists a neighborhood \mathcal{S} around \tilde{v}^* where all trajectories $\tilde{v}(t)$ satisfying (24) starting in \mathcal{S} converge to the set \tilde{V} whenever

$$\bar{\beta}_i < \sqrt{\tau_i D_i (4 - \tau_i l_i)}. \quad (26)$$

Moreover, the convergence of each such trajectory is to a point.

The proof of Theorem 5 is given in Appendix.D. In fact, the range of $\beta(t)$ can be very large as long as l_i is small enough. For example, set $\tau_i = 3/l_i$, then $\bar{\beta}_i(t) < \sqrt{3D_i/l_i}$. As we know, if we change the objective function to $k \sum_{i \in \mathcal{N}_{CG}} f_i(P_i^g)$, $k > 0$, the optimal solution will not change. Thus, l_i can be very small as long as k is small enough. In this regard, (26) is not conservative. Moreover, we will illustrate in Section VII that even (9) is binding, our controller still works.

VII. SIMULATION RESULTS

A. Test System

To test the proposed controller, the New England 39-bus system with 10 generators as shown in Fig.2, is utilized. In the simulation, we apply (23) to estimate the virtual load demands. All simulations are implemented in the commercial power system simulation software PSCAD [25], and are carried on a notebook with 8GB memory and 2.39 GHz CPU.

We control only a subset of these generators, namely G32, G36, G38, G39, while the remaining are equipped with the primary frequency control given in (14). In particular, we apply the controller (13) derived based on a simple model to a much more realistic and complicated model in PSCAD. The detailed electromagnetic transient model of three-phase synchronous machines (sixth-order model) is adopted to simulate generators with governors and exciters. All the lines and transformers take both resistance and reactance into account. The loads are modeled as fixed loads in PSCAD. The communication graph is undirected and set as $G32 \leftrightarrow G36 \leftrightarrow G38 \leftrightarrow G39 \leftrightarrow G32$.

The objective function is set as $f_i = \frac{1}{2}a_i(P_i^g)^2 + b_iP_i^g$, which is the generation cost of generator i . Capacity limits of P_i^g and parameters a_i, b_i are given in Table I.

The closed-loop system is shown in Fig.3, where each generator only needs to measure local frequency, mechanical power, voltage and phase angle to compute its control command. Note that there is no load measurement and only μ_i are communicated between neighboring controllable generators.

B. Results under Small Disturbances

We consider the following scenario: 1) at $t = 10$ s, there is a step change of 60MW load demands at each of buses 3, 15, 23, 24, 25; 2) at $t = 70$ s, there is another step change of 120MW load at bus 23. Neither the original load demands nor their changes are known to the generators.

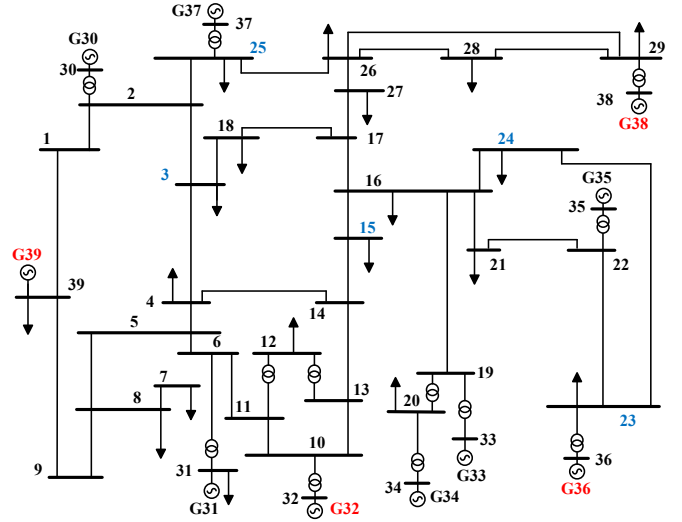


Fig. 2. The New England 39-bus system

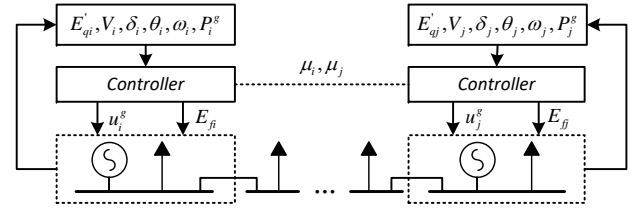


Fig. 3. Diagram of the closed-loop system

TABLE I
CAPACITY LIMITS OF GENERATORS

G_i	$[P_i^g, \bar{P}_i^g]$ (MW)	a_i	b_i
32	[0, 1000]	0.00009	0.032
36	[0, 1000]	0.00014	0.030
38	[0, 850]	0.00010	0.032
39	[0, 1080]	0.00008	0.032

TABLE II
EQUILIBRIUM POINTS

	P_{32}^g (MW)	P_{36}^g (MW)	P_{38}^g (MW)	P_{39}^g (MW)
Stage 1	927	610	834	1043
Stage 2	968	652	850	1080

1) *Equilibrium:* In steady states, the nominal frequency is well recovered. The optimal mechanical powers are given in Table II, which are identical to the optimal solution of (8) computed by centralized optimization. Stage 1 is for the period from 10s to 70s, and Stage 2 from 70s to 130s. The values in Table II are generations at the end of each stage. In Stage 1, no generation reaches its limit, while in Stage 2 both G38 and G39 reach their upper limits. At the end of each stage, the marginal generation cost $-\mu_i$ of generator i , converges identically (see Fig. 9), implying the optimality of the results. The test results confirm the theoretical analyses and demonstrate that our controller can automatically attain optimal operation points even in the more realistic and sophisticated model.

2) *Dynamic Performance:* In this subsection, we analyze the dynamic performance of the closed-loop system. For

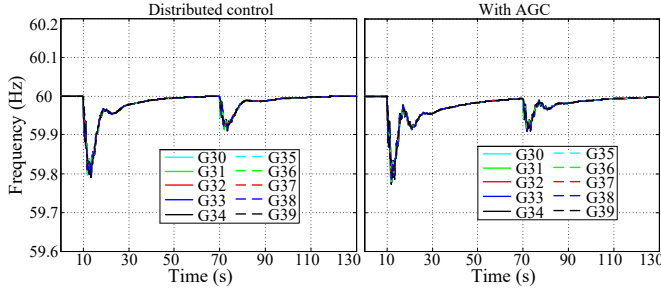


Fig. 4. Dynamics of frequencies

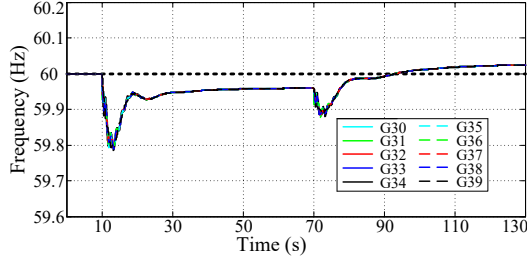


Fig. 5. Dynamics of frequencies with the controller in [11]

comparison, automatic generation control (AGC) is tested in the same scenario. In the AGC implementation, the signal of area control error (ACE) is given by $ACE = K_f \omega + P_{ij}$ [26, Chapter 11.6], where, K_f is the frequency response coefficient; ω the frequency deviation; P_{ij} the deviation of tie line power. In the case studies, we can treat the whole system as one control area, implying $P_{ij} = 0$. Hence, the control center computes $ACE = K_f \omega$ and allocates it to AGC generators, G32, G36, G38 and G39. In this situation, the control command of each generator is $r_i \cdot ACE$, where $\sum_i r_i = 1$. In this paper, we set $r_i = 0.25$ for $i = 1, 2, 3, 4$.

The trajectories of frequencies are given in Fig.4, where the left one stands for the proposed controller and the right one for the AGC. It is shown in Fig.4 that the frequencies are recovered to the nominal value under both controls. The frequency drops under two controls are very similar while the recovery time under the proposed control is much less than that under the conventional AGC.

Although a number of studies have been devoted to distributed frequency control of power systems, most of them assume that all the nodes are controllable except [11]. To make a fair comparison, the controller proposed in [11] is adopted as a rival in our tests. As shown in Eq.(8) of [11], each controller needs to predict the load it should supply in steady state. However, it is hard to acquire an accurate prediction in practice, which could lead to steady-state frequency error.

In the next case, we compare the two controls in the same scenario as that in Section VII.B. The dynamics of frequencies with the controller given in [11] are shown in Fig.5. It is observed that there is a frequency deviation in steady state, as the prediction is inaccurate. Although the deviation is usually quite small, it is difficult to completely eliminate. In contrast, when the proposed method is adopted, there is no frequency deviation in steady state, as is shown in Fig.4. This result is

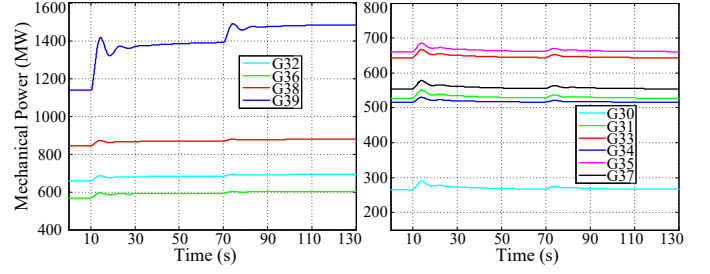


Fig. 6. Dynamics of mechanical powers under AGC

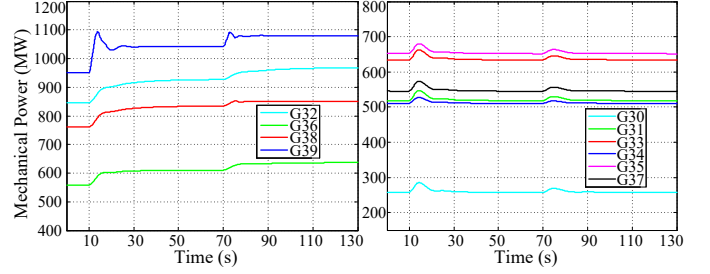


Fig. 7. Dynamics of mechanical powers under the proposed control

perfectly in coincidence with the indication given by Theorems 2, 3 and 5 and Lemma 4 in this paper.

Mechanical power dynamics under the AGC and the proposed controller are shown in Fig.6 and Fig.7, respectively. The left parts show mechanical powers of G32, G36, G38, G39, while the right parts show mechanical powers of other generators adopting conventional controller (14). With both controls, mechanical powers of the generators adopting (14) remain identical in the steady state. However, there are two problems when adopting the AGC: 1) mechanical powers are not optimal; 2) mechanical power of G39 violates the capacity limit. In contrast, the proposed control can avoid these problems. In Stage 1 of Fig.7, no generator reaches capacity limits. In Stage 2, both G38 and G39 reach their upper limits. Then, G38 and G39 stop increasing their outputs while G32 and G36 raise their outputs to balance the load demands. In addition, the steady states of in both stages are optimal, which are the same as shown in Table II.

We also illustrate in Fig.8 the dynamics of voltage at buses 3, 15, 23, 24, 25. The voltages converge rapidly, and only experience small drops when loads increase. This result validates the effectiveness of the voltage control.

The marginal generation cost of generator i , $-\mu_i$, are shown

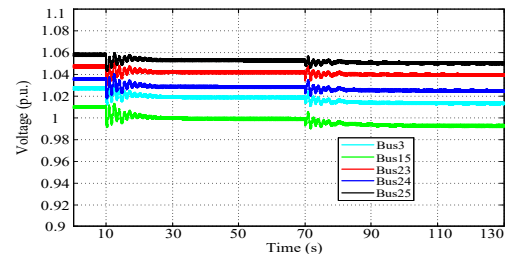


Fig. 8. Dynamics of bus voltages

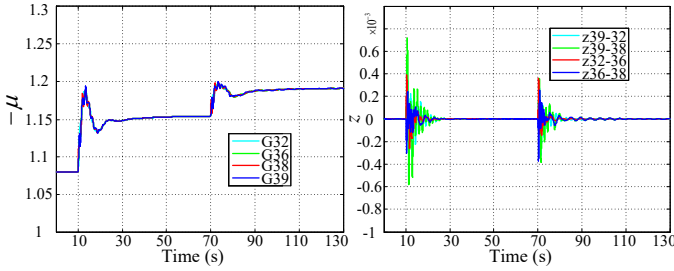
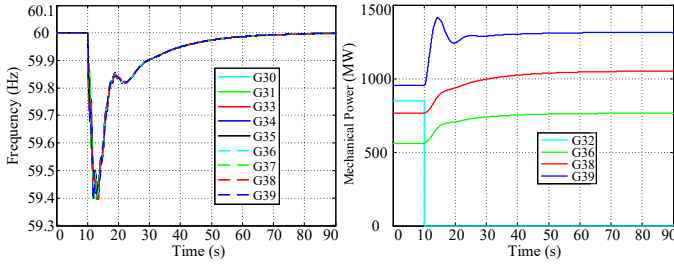

 Fig. 9. Dynamics of $-\mu$ and z


Fig. 10. Dynamics of frequencies and mechanical powers with generator trip

in the left part of Fig.9. They converge in both stages and the steady-state values in Stage 2 are slightly bigger than that in Stage 1, as the load changes lead to an increase in the marginal generation cost. Dynamics of z_{ij} , $(i, j) \in E$ are illustrated in the right part of Fig.9, which demonstrate that the steady state values do not change in the two stages. In addition, the variation of z in transient is very small as the deviation of μ_i is very small.

C. Performance under Large Disturbances

In this subsection, two scenarios of large disturbances are considered. One is a generator tripping and the other is a short-circuit fault followed by a line tripping.

1) *Generator tripping*: At $t = 10s$, G32 is tripped, followed by occurrence of certain power imbalance. Note that the communication graph still remains connected. The output of G32 drops to zero. Frequency and mechanical powers change accordingly. System dynamics are illustrated in Fig.10. The left part of Fig.10 shows the frequency dynamics, and the right shows the mechanical power dynamics of controllable generators. It is observed that the system frequency experiences a big drop at first, and then recovers to the nominal value quickly as other controllable generators increase outputs to balance the power mismatch. These results confirm that our controller can adapt to generator tripping autonomously even if the tripped generator is contributing to frequency control.

2) *Short-circuit fault*: At $t = 10s$, there occurs a three-phase short-circuit fault on line (4, 14). At $t = 10.05s$, this line is tripped by breakers. At $t = 60s$, the fault is removed and line (4, 14) is re-closed. Frequency dynamics and voltage dynamics of buses 4 and 14 are given in Fig.11, where the left part shows frequency dynamics and the right shows voltage dynamics. It can be seen that the frequency experiences violent oscillations after the fault happens. And then it is stabilized quickly once the line is tripped. Small frequency oscillation occurs when the

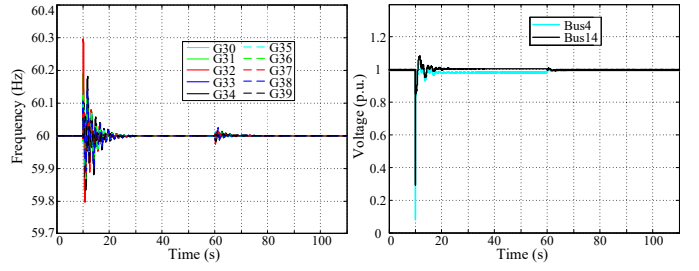
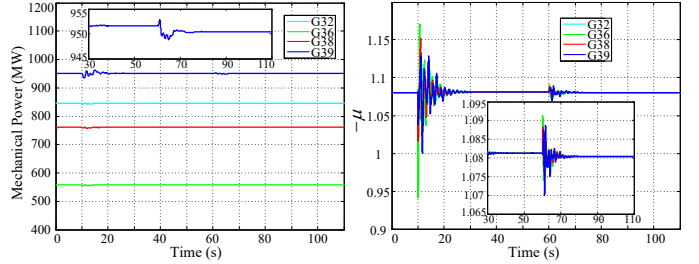


Fig. 11. Dynamics of frequencies and voltages with line trip


 Fig. 12. Dynamics of $-\mu$ and mechanical powers with line trip

line is re-closed. At the same time, the voltages of buses 4 and 14 drop to nearly zero when the fault happens. The voltages are then stabilized to a new steady-state value in around 10s after the fault line is tripped. They are slightly different from their initial values because the systems operating point has changed due to line tripping. When the tripped line is re-closed, the voltages recover to the initial values quickly.

When line (4, 14) is tripped, the power flow across the power network varies accordingly. As a consequence, the line loss also changes, causing variations of mechanical powers, as shown in Fig.12. In the left part of Fig.12, the inset is the dynamics of mechanical power of G39 from 30s to 110s. Similarly, the inset in the right part is dynamics of $-\mu$ of all generators. Mechanical powers and their marginal costs all increase when the line is tripped. However, the proposed controller compensates the loss change autonomously.

These simulation results demonstrate that the proposed distributed optimal frequency controller can cope with large disturbances such as generator tripping and short-circuit fault.

VIII. CONCLUSION

In this paper, we have designed a distributed optimal frequency control using a nonlinear network-preserving model, where only a subset of generator buses is controlled. We have also simplified the implementation by relaxing the requirements of load measurements and communication topology. Since nonlinearity of power flow model and dynamics of excitation voltage has been taken into account, our controllers can cope with large disturbances. We have proved that the closed-loop system asymptotically converges to the optimal solution of the economic dispatch problem. We have also carried out substantial simulations to verify the good performance of our controller under both small and large disturbances.

In this work, we have not considered the constraints on line flows, since the controllable generators are selected arbi-

trarily and may not suffice for congestion management. An interesting problem is how to find out the minimal set of controllable generators to fulfill the requirement of congestion management, which is our future work.

REFERENCES

- [1] D. Cai, E. Mallada, and A. Wierman, "Distributed optimization decomposition for joint economic dispatch and frequency regulation," *IEEE Trans. Power Syst.*, early access, 2017.
- [2] D. J. Shiltz, S. Baros, M. Cvetkovi?, and A. M. Annaswamy, "Integration of automatic generation control and demand response via a dynamic regulation market mechanism," *IEEE Trans. Control Syst. Technology*, vol. PP, no. 99, pp. 1–16, 2017.
- [3] A. Joki?, M. Lazar, and P. P. van den Bosch, "Real-time control of power systems using nodal prices," *Int. J. Elect. Power Energy Syst.*, vol. 31, no. 9, pp. 522–530, 2009.
- [4] F. Dorfler, J. W. Simpson-Porco, and F. Bullo, "Breaking the hierarchy: Distributed control and economic optimality in microgrids," *IEEE Trans. Control Netw. Syst.*, vol. 3, no. 3, pp. 241–253, Sept 2016.
- [5] N. Li, C. Zhao, and L. Chen, "Connecting automatic generation control and economic dispatch from an optimization view," *IEEE Trans. Control Netw. Syst.*, vol. 3, no. 3, pp. 254–264, Sept 2016.
- [6] D. Feijer and F. Paganini., "Stability of primal-dual gradient dynamics and applications to network optimization," *Automatica*, vol. 46, no. 12, pp. 1974–1981, Dec 2010.
- [7] C. Zhao, U. Topcu, N. Li, and S. H. Low., "Design and stability of load-side primary frequency control in power systems," *IEEE Trans. Autom. Control*, vol. 59, no. 5, pp. 1177–1189, Jan. 2014.
- [8] E. Mallada, C. Zhao, and S. H. Low, "Optimal load-side control for frequency regulation in smart grids," *IEEE Trans. Autom. Control*, early access, 2017.
- [9] A. Kasis, E. Devane, C. Spanias, and I. Lestas, "Primary frequency regulation with load-side participation part i: stability and optimality," *IEEE Trans. Power Syst.* early access, 2016.
- [10] C. Zhao, E. Mallada, S. Low, and J. Bialek, "A unified framework for frequency control and congestion management," in *Power Systems Computation Conference (PSCC)*, 2016. IEEE, 2016, pp. 1–7.
- [11] J. Z. Pang, L. Guo, and S. H. Low, "Load-side frequency regulation with limited control coverage," *ACM SIGMETRICS Performance Evaluation Review*, vol. 45, no. 2, pp. 94–96, 2017.
- [12] Z. Wang, F. Liu, S. H. Low, C. Zhao, and S. Mei, "Decentralized optimal frequency control of interconnected power systems with transient constraints," in *Proc. 55th IEEE Conf. Decis. Control (CDC)*, Dec 2016, pp. 664–671.
- [13] X. Zhang, N. Li, and A. Papachristodoulou, "Achieving real-time economic dispatch in power networks via a saddle point design approach," in *2015 IEEE PES General Meeting*, July 2015, pp. 1–5.
- [14] Z. Wang, F. Liu, S. H. Low, C. Zhao, and S. Mei, "Distributed frequency control with operational constraints, part i: Per-node power balance," *IEEE Trans. Smart Grid*, early access, 2017.
- [15] —, "Distributed frequency control with operational constraints, part ii: Network power balance," *IEEE Trans. Smart Grid*, early access, 2017.
- [16] T. Stegink, C. D. Persis, and A. van der Schaft, "A port-hamiltonian approach to optimal frequency regulation in power grids," in *54th IEEE Conference on Decision and Control (CDC)*, Dec 2015, pp. 3224–3229.
- [17] T. W. Stegink, C. De Persis, and A. J. van der Schaft, "Stabilization of structure-preserving power networks with market dynamics," *arXiv preprint arXiv:1611.04755*, 2016.
- [18] T. Stegink, C. D. Persis, and A. van der Schaft, "A unifying energy-based approach to stability of power grids with market dynamics," *IEEE Trans. Autom. Control*, vol. 62, no. 6, pp. 2612–2622, June 2017.
- [19] X. Zhang and A. Papachristodoulou., "A real-time control framework for smart power networks: Design methodology and stability," *Automatica*, vol. 58, pp. 43–50, Aug 2015.
- [20] C. Zhao and S. Low, "Optimal decentralized primary frequency control in power networks," in *Proc. 53rd IEEE Conf. Decis. Control (CDC)*, Dec 2014, pp. 2467–2473.
- [21] S. Trip and C. De Persis, "Optimal generation in structure-preserving power networks with second-order turbine-governor dynamics," in *Control Conference (ECC)*, 2016 European. IEEE, 2016, pp. 916–921.
- [22] P. Kundur, *Power System Stability and Control*. McGraw-hill New York, 1994, vol. 7.
- [23] Y. Liu, C. Li, and Y. Wang, "Decentralized excitation control of multi-machine multi-load power systems using hamiltonian function method," *Acta Automatica Sinica*, vol. 35, no. 7, pp. 919–925, 2009.

- [24] H. K. Khalil, *Nonlinear systems*. Prentice hall New Jersey, 1996, vol. 3.
- [25] <https://hvdc.ca/pscad/>.
- [26] V. V. Arthur and R. Bergen, *Power System Analysis*. Upper Saddle River: NJ: Prentice Hall, 2000.
- [27] S. Boyd and L. Vandenberghe, *Convex optimization*. Cambridge university press, 2004.
- [28] C. D. Persis, N. Monshizadeh, J. Schiffer, and F. Drfler, "A lyapunov approach to control of microgrids with a network-preserved differential-algebraic model," in *2016 IEEE 55th Conference on Decision and Control (CDC)*, Dec 2016, pp. 2595–2600.
- [29] P. Lin, Y. Jia, and L. Li, "Distributed robust h ∞ consensus control in directed networks of agents with time-delay," *Syst. Control Lett.*, vol. 57, no. 8, pp. 643–653, 2008.

APPENDIX

A. Proof of Theorem 2

Proof. From $\dot{\gamma}_i^- = \dot{\gamma}_i^+ = 0$ in (13d), it follows that $\underline{P}_i^g \leq P_i^{g*} \leq \bar{P}_i^g$, which is the first assertion. From $\dot{z}_{ij} = 0$ in (13c), we get $\mu_i^* = \mu_j^* = \mu_0$. Set $\dot{\mu}_i = 0$, add (13b) for $i \in \mathcal{N}_{CG}$, and recall $\sum_{i \in \mathcal{N}_{CG}} \tilde{p}_i = \sum_{i \in \mathcal{N}} p_i - \sum_{i \in \mathcal{N}_{UG}} P_i^{g*}$, we have

$$\sum_{i \in \mathcal{N}_{CG}} P_i^{g*} - \sum_{i \in \mathcal{N}} p_i + \sum_{i \in \mathcal{N}_{UG}} P_i^{g*} = 0 \quad (\text{A.1})$$

The right sides of (7a) and (7b) vanish in the equilibrium points, which implies $\omega_i^* = \tilde{\omega}_i^* = \tilde{\omega}_j^* = \omega_0$. Set $\dot{\omega}_i = 0$ and add (2b), (6b) and (6c). We have

$$\omega_0 \sum_{i \in \mathcal{N}} \tilde{D}_i = \sum_{i \in \mathcal{N}_{CG}} P_i^{g*} - \sum_{i \in \mathcal{N}} p_i + \sum_{i \in \mathcal{N}_{UG}} P_i^{g*} = 0 \quad (\text{A.2})$$

This implies that $\omega_0 = 0$ due to $\tilde{D}_i > 0$, which is the second assertion.

Combine (13a), (2d) and $\dot{P}_i^g = 0$. We have

$$f'_i(P_i^{g*}) - \gamma_i^{-*} + \gamma_i^{+*} + \omega_i^* + \mu_i^* = 0$$

Since $\omega_0 = 0$, $\mu_i^* = \mu_j^* = \mu_0$, we can obtain the third assertion.

Next we will prove assertion 4). Since all the constraints of SFC are linear, A3 implies that Slater's condition holds [27, Chapter 5.2.3]. Moreover, the objective function is strictly convex. We only need to prove that $(P_i^{g*}, \mu_0, \gamma_i^{-*}, \gamma_i^{+*})$ satisfies the KKT condition of SFC in order to prove the fourth assertion.

The KKT conditions of SFC problem (8) are

$$f'_i(P_i^{g*}) - \gamma_i^{-*} + \gamma_i^{+*} + \mu_0 = 0 \quad (\text{A.3a})$$

$$\sum_{i \in \mathcal{N}_{CG}} P_i^{g*} - \sum_{i \in \mathcal{N}} p_i + \sum_{i \in \mathcal{N}_{UG}} P_i^{g*} = 0 \quad (\text{A.3b})$$

$$\underline{P}_i^g \leq P_i^{g*} \leq \bar{P}_i^g \quad (\text{A.3c})$$

$$\gamma_i^{-*} \geq 0, \gamma_i^{+*} \geq 0 \quad (\text{A.3d})$$

$$\gamma_i^{-*}(\underline{P}_i^g - P_i^{g*}) = 0, \gamma_i^{+*}(P_i^{g*} - \bar{P}_i^g) = 0 \quad (\text{A.3e})$$

From $\dot{\gamma}_i^- = \dot{\gamma}_i^+ = 0$, we have (A.3c), (A.3d) and (A.3e). From the third assertion, we have (A.3a). From $\dot{\omega} = 0$ and the second assertion, we have (A.3b). Therefore, the equilibrium points of the closed-loop system (16) satisfy the KKT conditions (A.3). This implies the fourth assertion.

If A3 is strictly satisfied, we know $\exists i \in \mathcal{N}_{CG}$ that $\gamma_i^{-*} = \gamma_i^{+*} = 0$. Then, $\mu_i^* = -f'_i(P_i^{g*})$ is uniquely determined by P_i^{g*} , implying the last assertion. This completes the proof. \square

B. Proof of Theorem 3

Proof of Theorem 3. Recall (18), and dynamics of (13a) - (13e) are rewritten as

$$\dot{P}_i^g = -k_{P_i^g} \cdot \left(\omega_i + \partial \hat{L}(x_1, x_2) / \partial P_i^g \right) \quad (\text{B.1a})$$

$$\dot{\mu}_i = k_{\mu_i} \cdot \partial \hat{L}(x_1, x_2) / \partial \mu_i \quad (\text{B.1b})$$

$$\dot{z}_{ij} = k_{z_{ij}} \cdot \partial \hat{L}(x_1, x_2) / \partial z_{ij} \quad (\text{B.1c})$$

$$\dot{\gamma}_i^- = k_{\gamma_i^-} \cdot \left[\partial \hat{L}(x_1, x_2) / \partial \gamma_i^- \right]_{\gamma_i^-}^+ \quad (\text{B.1d})$$

$$\dot{\gamma}_i^+ = k_{\gamma_i^+} \cdot \left[\partial \hat{L}(x_1, x_2) / \partial \gamma_i^+ \right]_{\gamma_i^+}^+ \quad (\text{B.1e})$$

With regard to the closed-loop system, we first define two sets, σ^+ and σ^- , as follows [6].

$$\sigma^+ := \{i \in \mathcal{N}_{CG} \mid \gamma_i^+ = 0, P_i^g - \bar{P}_i^g < 0\} \quad (\text{B.2a})$$

$$\sigma^- := \{i \in \mathcal{N}_{CG} \mid \gamma_i^- = 0, \underline{P}_i^g - P_i^g < 0\} \quad (\text{B.2b})$$

Then (13d) and (13e) are equivalent to

$$\dot{\gamma}_i^+ = \begin{cases} k_{\gamma_i^+} (P_i^g - \bar{P}_i^g), & \text{if } i \notin \sigma^+; \\ 0, & \text{if } i \in \sigma^+. \end{cases} \quad (\text{B.3a})$$

$$\dot{\gamma}_i^- = \begin{cases} k_{\gamma_i^-} (\underline{P}_i^g - P_i^g), & \text{if } i \notin \sigma^-; \\ 0, & \text{if } i \in \sigma^-. \end{cases} \quad (\text{B.3b})$$

The derivative of W_k is

$$\begin{aligned} \dot{W}_k &= \sum_{i \in \mathcal{N}_G} M_i (\omega_i - \omega_i^*) \dot{\omega}_i + (x - x^*)^T \cdot K^{-1} \dot{x} \\ &\leq \sum_{i \in \mathcal{N}_G} (\omega_i - \omega_i^*) (P_i^g - D_i \omega_i - P_{ei}) - \sum_{i \in \mathcal{N}_{CG}} (P_i^g - P_i^{g*}) \omega_i \\ &\quad - (x_1 - x_1^*)^T \cdot \nabla_{x_1} \hat{L} + (x_2 - x_2^*)^T \cdot \nabla_{x_2} \hat{L} \\ &= \sum_{i \in \mathcal{N}_G} (\omega_i - \omega_i^*) (P_i^g - P_i^{g*} - D_i (\omega_i - \omega_i^*) - (P_{ei} - P_{ei}^*)) \\ &\quad - \sum_{i \in \mathcal{N}_{CG}} (P_i^g - P_i^{g*}) \cdot (\omega_i - \omega_i^*) \\ &\quad - (x_1 - x_1^*)^T \cdot \nabla_{x_1} \hat{L} + (x_2 - x_2^*)^T \cdot \nabla_{x_2} \hat{L} \\ &= -(x_1 - x_1^*)^T \cdot \nabla_{x_1} \hat{L} + (x_2 - x_2^*)^T \cdot \nabla_{x_2} \hat{L} \\ &\quad - \sum_{i \in \mathcal{N}_G} D_i (\omega_i - \omega_i^*)^2 - \sum_{i \in \mathcal{N}_G} (\omega_i - \omega_i^*) (P_{ei} - P_{ei}^*) \\ &\quad + \sum_{i \in \mathcal{N}_{UG}} (P_i^g - P_i^{g*}) (\omega_i - \omega_i^*) \end{aligned} \quad (\text{B.4})$$

where the inequality is due to

$$\begin{aligned} (\gamma^- - \gamma^{*-})^T [P^g - P^g]_{\gamma^-}^+ &\leq (\gamma^- - \gamma^{*-})^T (P^g - P^g) \\ &= (\gamma^- - \gamma^{*-})^T \nabla_{\gamma^-} \hat{L} \end{aligned}$$

Here the inequality holds since $\gamma_i^- = 0 \leq \gamma_i^{*-}$ and $\underline{P}_i^g - P_i^g < 0$ for $i \in \sigma^-$, i.e., $(\gamma_i^- - \gamma_i^{*-}) \cdot (P_i^g - P_i^g) \geq 0$. Similarly for $i \in \sigma^+$, we have

$$\begin{aligned} (\gamma^+ - \gamma^{*+})^T [P^g - \bar{P}^g]_{\gamma^+}^+ &\leq (\gamma^+ - \gamma^{*+})^T (P^g - \bar{P}^g) \\ &= (\gamma^+ - \gamma^{*+})^T \nabla_{\gamma^+} \hat{L} \end{aligned}$$

From (6b) and (6c), it yields

$$0 = \sum_{i \in \mathcal{N}_G} (\tilde{\omega}_i - \tilde{\omega}_i^*) \left((P_{ei} - P_{ei}^*) - \sum_{j \in \mathcal{N}_i} (P_{ij} - P_{ij}^*) \right) \quad (\text{B.5})$$

$$- \sum_{i \in \mathcal{N}} \tilde{D}_i (\tilde{\omega}_i - \tilde{\omega}_i^*)^2 - \sum_{i \in \mathcal{N}_L} (\tilde{\omega}_i - \tilde{\omega}_i^*) \sum_{j \in \mathcal{N}_i} (P_{ij} - P_{ij}^*)$$

Add (B.5) to (B.4), then we have

$$\begin{aligned} \dot{W}_k &\leq - \sum_{i \in \mathcal{N}_G} D_i (\omega_i - \omega_i^*)^2 - \sum_{i \in \mathcal{N}} \tilde{D}_i (\tilde{\omega}_i - \tilde{\omega}_i^*)^2 \\ &\quad + \sum_{i \in \mathcal{N}_G} (\tilde{\omega}_i - \omega_i) (P_{ei} - P_{ei}^*) - \sum_{(i,j) \in \mathcal{E}} (\tilde{\omega}_i - \tilde{\omega}_j) (P_{ij} - P_{ij}^*) \\ &\quad + \sum_{i \in \mathcal{N}_{UG}} (P_i^g - P_i^{g*}) (\omega_i - \omega_i^*) \\ &\quad - (x_1 - x_1^*)^T \cdot \nabla_{x_1} \hat{L} + (x_2 - x_2^*)^T \cdot \nabla_{x_2} \hat{L} \end{aligned} \quad (\text{B.6})$$

Since \hat{L} is a convex function of x_1 and a concave function of x_2 , we have

$$\begin{aligned} &-(x_1 - x_1^*)^T \cdot \nabla_{x_1} \hat{L}(x_1, x_2) + (x_2 - x_2^*)^T \cdot \nabla_{x_2} \hat{L}(x_1, x_2) \\ &\leq \hat{L}(x_1^*, x_2) - \hat{L}(x_1, x_2) + \hat{L}(x_1, x_2) - \hat{L}(x_1, x_2^*) \\ &= \hat{L}(x_1^*, x_2) - \hat{L}(x_1^*, x_2^*) + \hat{L}(x_1^*, x_2^*) - \hat{L}(x_1, x_2^*) \\ &\leq 0 \end{aligned} \quad (\text{B.7})$$

where the first inequality follows because \hat{L} is convex in x_1 and concave in x_2 and the second inequality follows because (x_1^*, x_2^*) is a saddle point. Hence, we have

$$\begin{aligned} \dot{W}_k &\leq - \sum_{i \in \mathcal{N}_G} D_i (\omega_i - \omega_i^*)^2 - \sum_{i \in \mathcal{N}} \tilde{D}_i (\tilde{\omega}_i - \tilde{\omega}_i^*)^2 \\ &\quad - \sum_{i \in \mathcal{N}_G} (\omega_i - \tilde{\omega}_i) (P_{ei} - P_{ei}^*) - \sum_{(i,j) \in \mathcal{E}} (\tilde{\omega}_i - \tilde{\omega}_j) (P_{ij} - P_{ij}^*) \\ &\quad + \sum_{i \in \mathcal{N}_{UG}} (P_i^g - P_i^{g*}) (\omega_i - \omega_i^*) \end{aligned} \quad (\text{B.8})$$

The partial of $W_p(x_p)$ is

$$\nabla_{E_{qi}'} W_p = \frac{1}{x_{di} - x_{di}'} (E_{qi} - E_{qi}^*) \quad (\text{B.9a})$$

$$\nabla_{V_i} W_p = 0 \quad (\text{B.9b})$$

$$\nabla_{\delta_i} W_p = P_{ei} - P_{ei}^* \quad (\text{B.9c})$$

$$\nabla_{\theta_i} W_p = \sum_{(i,j) \in \mathcal{E}} (P_{ij} - P_{ij}^*) - \sum_{i \in \mathcal{N}_G} (P_{ei} - P_{ei}^*) \quad (\text{B.9d})$$

The derivative of W_p is

$$\begin{aligned} \dot{W}_p &= \sum_{i \in \mathcal{N}_G} \frac{(E_{qi} - E_{qi}^*) (E_{fi} - E_{fi}^*)}{T_{d0i}' (x_{di} - x_{di}')} - \sum_{i \in \mathcal{N}_G} \frac{(E_{qi} - E_{qi}^*)^2}{T_{d0i}' (x_{di} - x_{di}')} \\ &\quad + \sum_{i \in \mathcal{N}_G} (\omega_i - \tilde{\omega}_i) (P_{ei} - P_{ei}^*) + \sum_{(i,j) \in \mathcal{E}} (\tilde{\omega}_i - \tilde{\omega}_j) (P_{ij} - P_{ij}^*) \end{aligned} \quad (\text{B.10})$$

The Lyapunov function is defined as $W = W_k + W_p + \sum_{i \in \mathcal{N}_{UG}} S_{\omega_i} + \sum_{i \in \mathcal{N}_G} \frac{1}{T_{d0i}' (x_{di} - x_{di}')} S_{E_i}$, and its derivative is

$$\begin{aligned} \dot{W} &= \dot{W}_k + \dot{W}_p + \sum_{i \in \mathcal{N}_{UG}} \dot{S}_{\omega_i} + \sum_{i \in \mathcal{N}_G} \frac{\dot{S}_{E_i}}{T_{d0i}' (x_{di} - x_{di}')} \\ &\leq - \sum_{i \in \mathcal{N}_G} D_i (\omega_i - \omega_i^*)^2 - \sum_{i \in \mathcal{N}} \tilde{D}_i (\tilde{\omega}_i - \tilde{\omega}_i^*)^2 \\ &\quad - \sum_{i \in \mathcal{N}_G} \frac{(E_{qi} - E_{qi}^*)^2}{T_{d0i}' (x_{di} - x_{di}')} \end{aligned}$$

$$\begin{aligned}
 & + \sum_{i \in \mathcal{N}_{UG}} (P_i^g - P_i^{g*})(\omega_i - \omega_i^*) + \sum_{i \in \mathcal{N}_{UG}} \dot{S}_{\omega_i} \\
 & + \sum_{i \in \mathcal{N}_G} \frac{(E_{qi} - E_{qi}^*)(E_{fi} - E_{fi}^*)}{T_{d0i}(x_{di} - x'_{di})} + \sum_{i \in \mathcal{N}_G} \frac{\dot{S}_{E_i}}{T_{d0i}(x_{di} - x'_{di})} \\
 & \leq - \sum_{i \in \mathcal{N}_G} D_i(\omega_i - \omega_i^*)^2 - \sum_{i \in \mathcal{N}} \tilde{D}_i(\tilde{\omega}_i - \tilde{\omega}_i^*)^2 \\
 & - \sum_{i \in \mathcal{N}_G} \frac{(E_{qi} - E_{qi}^*)^2}{T_{d0i}(x_{di} - x'_{di})} - \sum_{i \in \mathcal{N}_{UG}} \phi_{\omega_i} - \sum_{i \in \mathcal{N}_G} \phi_{E_i} \\
 & \leq 0
 \end{aligned} \tag{B.11}$$

The last two inequalities are due to assumption A4.

To prove the locally asymptotic stability of the closed-loop system, we also need to prove that $W > 0, \forall v \in S \setminus v^*$. Equivalently, we need $\nabla_v^2 W > 0, \forall v \in S \setminus v^*$, i.e. A4.

Consequently, there exists a neighborhood set $\{v : W(v) \leq \epsilon\}$ for all sufficiently small $\epsilon > 0$ so that $\nabla_v^2 W(v) > 0$. Hence, there is a compact set \mathcal{S} around v^* contained in such neighborhood, which is forward invariant. Let $Z_1 := \{v : \dot{W}(v) = 0\}$. By LaSalle's invariance principle, the each of trajectories $v(t)$ starting from \mathcal{S} converges to the largest invariant set Z^+ contained in $\mathcal{S} \cap Z_1$. From above analysis, if $\dot{W}(v) = 0, v$ is an equilibrium point of the closed-loop system (16). Hence, v converges to $Z^+ \in \mathcal{V}$.

Finally, we will prove the convergence of each $v(t)$ starting from \mathcal{V} is to a point by following the proof of Theorem 1 in [18]. Since $v(t)$ is bounded, its ω -limit set $\Omega(v) \neq \emptyset$. By contradiction, suppose there exist two different points in $\Omega(v)$, i.e., $v_1^*, v_2^* \in \Omega(v), v_1^* \neq v_2^*$. Since the Hessian of $W_1(v), W_2(v)$ is positive definite in \mathcal{S} , there exist $W_1(v), W_2(v)$ defined by (22) with respect to v_1^*, v_2^* and scalars $c_1 > 0, c_2 > 0$ such that two sets $W_1^{-1}(\leq c_1) := \{v | W_1(v) \leq c_1\}, W_2^{-1}(\leq c_2) := \{v | W_2(v) \leq c_2\}$ are disjoint (i.e. $W_1^{-1}(\leq c_1) \cap W_2^{-1}(\leq c_2) = \emptyset$) and compact. In addition, $W_1^{-1}(\leq c_1), W_2^{-1}(\leq c_2)$ are forward invariant. By (B.11), there exists a finite time $t_1 > 0$ such that $v(t) \in W_1^{-1}(\leq c_1)$ for $\forall t \geq t_1$. Similarly, there exists a finite time $t_2 > 0$ such that $v(t) \in W_2^{-1}(\leq c_2)$ for $\forall t \geq t_2$. This implies that $v(t) \in W_1^{-1}(\leq c_1) \cap W_2^{-1}(\leq c_2)$ for $\forall t \geq \max(t_1, t_2)$, which is a contradiction. This completes the proof. \square

In this part, we discuss the reasonableness of Assumption A4 by referring to [28, Lemma 3]. Reference [28] investigates the control of inverter-based microgrids based on a network-preserving model, while we extend some results to more complicated synchronous-generator based bulk power systems. For simplicity, we first present some notations following [28]. Comparing (1) and (4), P_{ei}, Q_{ei} have same structures with P_{ij}, Q_{ij} , respectively. We can treat the reactance of generator as a line with admittance as $1/x'_{di}$, which connects $i \in \mathcal{N}_G$ and inner node of the generator. We denote the inner nodes of generators as \mathcal{N}'_G . Then, we can get a augmented power network, the incidence matrix of which is denoted as \hat{C} . The set of nodes in the augmented power network is denoted as $\mathcal{N}' = \mathcal{N} \cup \mathcal{N}'_G$. Denote $\hat{V} = (E'_q, V), \hat{\theta} = (\delta, \theta)$. Let $|\hat{C}|$ denote the matrix obtained from \hat{C} by replacing all the elements

c_{ij} with $|c_{ij}|$. Define $\Gamma(\hat{V}) := \text{diag}(|B_{ij}|V_iV_j), i, j \in \mathcal{N}'$. Define A as

$$A_{ij} = \begin{cases} -|B_{ij}| \cos(\theta_i - \theta_j), & i \neq j, i, j \in \mathcal{N}; \\ \text{diag}(|B_{ii}|), & i = j, i, j \in \mathcal{N}; \\ -\cos(\delta_i - \theta_j)/x'_{di}, & i \in \mathcal{N}'_G, j \in \mathcal{N}_G. \end{cases} \tag{B.12}$$

For simplicity, we use the following notation. For an n -dimensional vector $r := \{r_1, r_2, \dots, r_n\}$, the diagonal matrix $\text{diag}(r_1, r_2, \dots, r_n)$ is denoted in short by $[r]_{\mathcal{D}}$. And $\mathbf{cos}(\cdot), \mathbf{sin}(\cdot)$ are defined component-wise.

From the definition of W in (22), $\nabla_v^2 W(v) > 0$ if and only if $\nabla_v^2 W_p(v) > 0$, i.e. the matrix

$$\begin{bmatrix} \Gamma(\hat{V})[\mathbf{cos}(\hat{C}^T \hat{\theta})]_{\mathcal{D}} & [\mathbf{sin}(\hat{C}^T \hat{\theta})]_{\mathcal{D}} \Gamma(\hat{V}) |\hat{C}|^T [\hat{V}]_{\mathcal{D}}^{-1} \\ [\hat{V}]_{\mathcal{D}}^{-1} |\hat{C}| \Gamma(\hat{V}) [\mathbf{sin}(\hat{C}^T \hat{\theta})]_{\mathcal{D}} & A + H(\hat{V}) \end{bmatrix} \tag{B.13}$$

is positive definite, where

$$H(\hat{V}) = \begin{bmatrix} \left[\frac{x_{di}}{2x'_{di}(x_{di} - x'_{di})} \right]_{\mathcal{D}} & 0 \\ 0 & [q_i/V_i^2]_{\mathcal{D}} \end{bmatrix} \tag{B.14}$$

In any steady state of power system (i.e.), the phase-angle difference between two neighboring nodes is usually small. In addition, the difference between δ_i and θ_i is also small. This implies that the matrix in (B.13) is diagonal dominant as well as its positive definiteness. Therefore, Assumption A4 is usually satisfied and makes sense.

C. Proof of Lemma 4

Proof. From $\dot{z}_{ij} = 0$, we get $\mu_i^* = \mu_j^* = \mu_0$. Set $\dot{\mu}_i = 0$ and add (23) for $i \in \mathcal{N}_{CG}$, we have

$$\sum_{i \in \mathcal{N}_{CG}} M_i \dot{\omega}_i + \sum_{i \in \mathcal{N}_{CG}} (D_i + \tau_i) \omega_i = 0 \tag{C.1}$$

The right sides of (7a) and (7b) vanish in the equilibrium points, which implies $\omega_i^* = \tilde{\omega}_i^* = \tilde{\omega}_j^* = \omega_0$. Set $\dot{\omega} = 0$ in (C.1) and we have

$$\omega_0 \sum_{i \in \mathcal{N}_{CG}} (D_i + \tau_i) = 0 \tag{C.2}$$

This implies that $\omega_0 = 0$ due to $D_i + \tau_i > 0$.

Other proofs are same with that in Theorem 2, which are omitted. \square

D. Proof of Theorem 5

Proof of Theorem 5. We still use the Lyapunov function (22) to analyze the stability of the closed-loop system (24). Denote $y = (\omega_i^T, x_1^T, x_2^T)^T, i \in \mathcal{N}_{CG}$, and define the following function

$$\tilde{f}(y) = \begin{bmatrix} -D_i \omega_i \\ -\left(f'_i(P_i^g) + \mu_i - \gamma_i^- + \gamma_i^+ \right) \\ f_{\mu_i} \\ \mu_i - \mu_j \\ P_i^g - P_j^g \\ P_i^g - \bar{P}_i^g \end{bmatrix}, i \in \mathcal{N}_{CG} \tag{D.1}$$

where $f_{\mu_i} = P_i^g - \hat{p}_i - \sum_{j \in N_{ci}} (\mu_i - \mu_j) - \sum_{j \in N_{ci}} z_{ij} - \tau_i \mu_i - \tau_i f_i'(P_i^g) + \beta_i \omega_i^1$.

The derivative of W_k is

$$\begin{aligned} \dot{W}_k &= \sum_{i \in N_G} M_i (\omega_i - \omega_i^*) \dot{\omega}_i + (x - x^*)^T \cdot K^{-1} \dot{x} \\ &= \sum_{i \in N_G} (\omega_i - \omega_i^*) (P_i^g - P_i^{g*} - D_i (\omega_i - \omega_i^*) - (P_{ei} - P_{ei}^*)) \\ &\quad + (x - x^*)^T \cdot K^{-1} \dot{x} \\ &\leq \sum_{i \in N_G} (\omega_i - \omega_i^*) (P_i^g - P_i^{g*} - (P_{ei} - P_{ei}^*)) \\ &\quad - \sum_{i \in N_{UG}} D_i (\omega_i - \omega_i^*)^2 + (y - y^*)^T \tilde{f}(y) \end{aligned} \quad (\text{D.2})$$

where the inequality is due to the same reason for that in (B.4).

Divide \dot{W}_k into two parts, and $\dot{W}_k^1 = (y - y^*)^T \tilde{f}(y)$, $\dot{W}_k^2 = \dot{W}_k - \dot{W}_k^1$. Then we will analyze the sign of \dot{W}_k^1 .

$$\begin{aligned} \dot{W}_k^1 &= (y - y^*)^T \tilde{f}(y) \\ &= \int_0^1 (y - y^*)^T \frac{\partial}{\partial \tilde{z}} \tilde{f}(\tilde{z}(s)) (y - y^*) ds + (y - y^*)^T \tilde{f}(y^*) \\ &\leq \frac{1}{2} \int_0^1 (y - y^*)^T \left[\frac{\partial^T}{\partial \tilde{z}} \tilde{f}(\tilde{z}(s)) + \frac{\partial}{\partial \tilde{z}} \tilde{f}(\tilde{z}(s)) \right] (y - y^*) ds \\ &= \int_0^1 (y - y^*)^T [H(\tilde{z}(s))] (y - y^*) ds \end{aligned} \quad (\text{D.3})$$

where $\tilde{z}(s) = y^* + s(y - y^*)$. The second equation is from the fact that $\tilde{f}(y) - \tilde{f}(y^*) = \int_0^1 \frac{\partial}{\partial \tilde{z}} \tilde{f}(\tilde{z}(s)) (y - y^*) ds$. The inequality is due to either $\tilde{f}(y^*) = 0$ or $\tilde{f}(y^*) < 0, y_i \geq 0$, i.e. $(y - y^*)^T \tilde{f}(y^*) \leq 0$.

$$\frac{\partial \tilde{f}(y)}{\partial y} = - \begin{bmatrix} D & 0 & 0 & 0 & 0 & 0 \\ 0 & \nabla_{P^g}^2 f(P^g) & I & 0 & -I & I \\ \beta & \tau \nabla_{P^g}^2 f(P^g) - I & \tau + L_c & C & 0 & 0 \\ 0 & 0 & -C^T & 0 & 0 & 0 \\ 0 & I & 0 & 0 & 0 & 0 \\ 0 & -I & 0 & 0 & 0 & 0 \end{bmatrix} \quad (\text{D.4})$$

where $D = \text{diag}(D_i)$, $\beta = \text{diag}(\beta_i)$, $\tau = \text{diag}(\tau_i)$, I is the identity matrix with dimension n_{CG} , C is the incidence matrix of the communication graph, L_c is the Laplacian matrix of the communication graph.

Finally, H in (D.3) is

$$\begin{aligned} H &= \frac{1}{2} \left[\frac{\partial^T}{\partial y} \tilde{f}(y) + \frac{\partial}{\partial y} \tilde{f}(y) \right] \\ &= \begin{bmatrix} -D & 0 & -\frac{1}{2}\beta & 0 & 0 & 0 \\ 0 & -\nabla_{P^g}^2 f(P^g) & -\frac{\tau}{2} \nabla_{P^g}^2 f(P^g) & 0 & 0 & 0 \\ -\frac{1}{2}\beta & -\frac{\tau}{2} \nabla_{P^g}^2 f(P^g) & -\tau - L_c & 0 & 0 & 0 \\ 0 & 0 & 0 & 0 & 0 & 0 \\ 0 & 0 & 0 & 0 & 0 & 0 \\ 0 & 0 & 0 & 0 & 0 & 0 \end{bmatrix} \end{aligned} \quad (\text{D.5})$$

¹Sometimes, we also use β_i instead of $\beta_i(t)$ for simplification. In addition, if (9) is not binding, we can omit γ_i^-, γ_i^+ in neighborhoods of equilibrium points

$H \leq 0$, if

$$\begin{bmatrix} -D & 0 & -\frac{1}{2}\beta \\ 0 & -\nabla_{P^g}^2 f(P^g) & -\frac{\tau}{2} \nabla_{P^g}^2 f(P^g) \\ -\frac{1}{2}\beta & -\frac{\tau}{2} \nabla_{P^g}^2 f(P^g) & -\tau \end{bmatrix} < 0 \quad (\text{D.6})$$

By Schur complement [29], we only need

$$-\tau_i - \begin{bmatrix} -\frac{1}{2}\beta_i & -\frac{\tau_i}{2} c_i \end{bmatrix} \begin{bmatrix} -D_i & 0 \\ 0 & -c_i \end{bmatrix}^{-1} \begin{bmatrix} -\frac{1}{2}\beta_i \\ -\frac{\tau_i}{2} c_i \end{bmatrix} < 0 \quad (\text{D.7})$$

where $c_i = \nabla_{P_i^g}^2 f(P_i^g)$. Solving (D.7), we can get

$$-\sqrt{\tau_i D_i (4 - \tau_i c_i)} < \beta_i < \sqrt{\tau_i D_i (4 - \tau_i c_i)} \quad (\text{D.8})$$

By A2, we know $c_i \leq l_i$, thus

$$\begin{aligned} \sqrt{\tau_i D_i (4 - \tau_i l_i)} &\leq \sqrt{\tau_i D_i (4 - \tau_i c_i)}, \\ -\sqrt{\tau_i D_i (4 - \tau_i l_i)} &\geq -\sqrt{\tau_i D_i (4 - \tau_i c_i)}. \end{aligned}$$

Here we need $\tau_i > 0$, $4 - \tau_i l_i > 0$, i.e. $0 < \tau_i < 4/l_i$. Finally, we have

$$-\sqrt{\tau_i D_i (4 - \tau_i l_i)} < \beta_i < \sqrt{\tau_i D_i (4 - \tau_i l_i)} \quad (\text{D.9})$$

i.e. $\beta_i < \sqrt{\tau_i D_i (4 - \tau_i l_i)}$, implying (26).

Analysis of \dot{W}_k^2 and \dot{W}_p as well as the convergence to a point are same as those in the proof of Theorem 3, which are omitted here. \square